Supplementary information

Color-coded galectin fusion proteins as novel tools in biomaterial science

Carina Dey, [a] Isabel K. Sommerfeld,[b,c] Pavla Bojarová,[d,e] Nikol Kodra[a], David Vrbata,[d] Miluše Zimolová Vlachová,[d] Vladimír Křen,[d] Andrij Pich [b,c,f] and Lothar Elling*[a]

[a]Laboratory for Biomaterials, Institute for Biotechnology and Helmholtz-Institute for Biomedical Engineering, RWTH Aachen University, Pauwelsstraße 20, 52074 Aachen, Germany.
[b]DWI − Leibniz-Institute for Interactive Materials e.V. Forckenbeckstr. 50, 52074 Aachen
[c]Functional and Interactive Polymers, Institute of Technical and Macromolecular Chemistry, RWTH Aachen University, Worringerweg 2, 52074 Aachen.
[d]Laboratory of Biotransformation, Institute of Microbiology of the Czech Academy of Sciences, Vídeňská 1083, Prague 4, 14200, Czech Republic.
[e]Department of Health Care Disciplines and Population Protection, Faculty of Biomedical Engineering, Czech Technical University in Prague, nám. Sítná 3105, 27201 Kladno, Czech Republic.
[f]Aachen Maastricht Institute for Biobased Materials (AMIBM), Maastricht University, Brightlands Chemelot Campus, Urmonderbaan 22, 6167 RD Geleen, The Netherlands

* Correspondence: l.elling@biotec.rwth-aachen.de; Tel.: +49 241 8028350

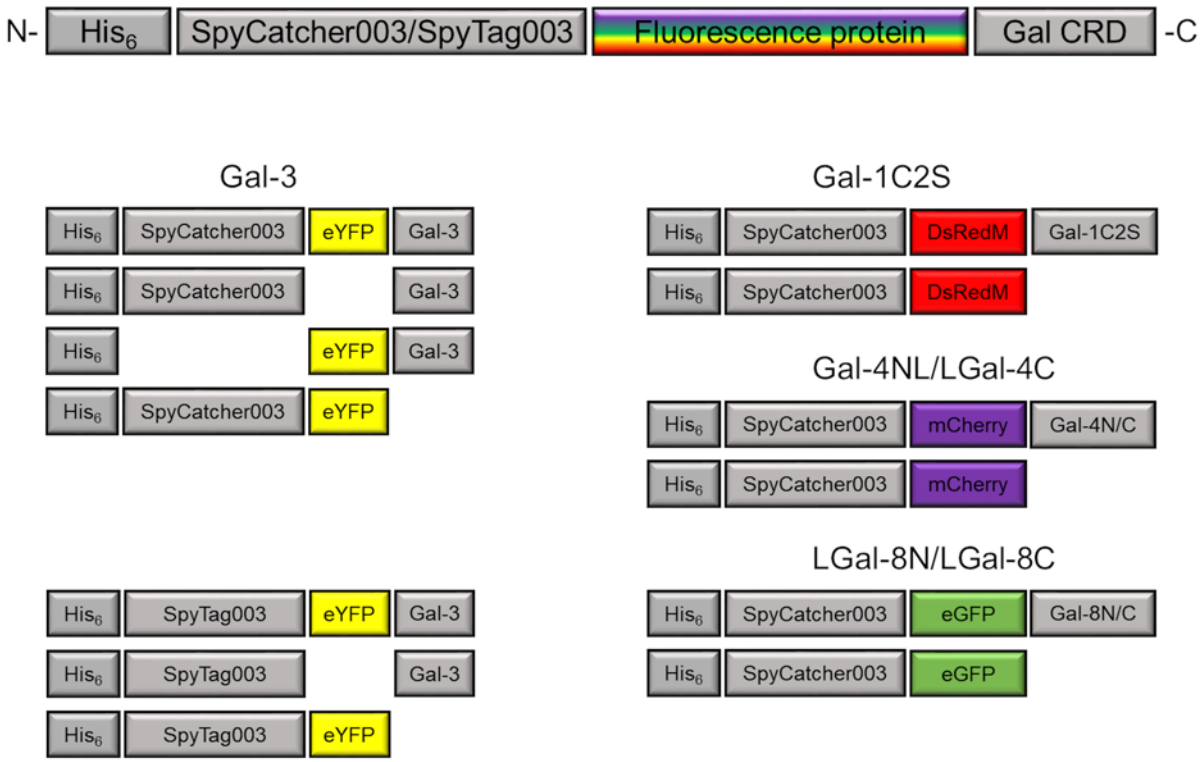

Scheme S1. Schematic structure of SpyCatcher and SpyTag galectin fusion proteins used in this study. Full-length sequences of Gal-1C2S and Gal-3 genes were utilized for the construction of the respective fusion gene constructs. Fusion proteins of Gal-4 and Gal-8 comprised the respective subdomains along with the segment of the linker peptide. Specifically, Gal-4NL corresponds to amino acids 1-160 of Gal-4, while LGal-4C corresponds to the amino acids 169-323 of full-length Gal-4. Gal-8NL corresponds to amino acids 1-160 of the full-length Gal-8 (isoform b), while LGal-8C corresponds to amino acids 182-317 of the full-length Gal-8 (isoform b).

Table S1: Abbreviations used in this study.

Abbreviation	Description
CRD	Carbohydrate recognition domain
H	His_6-tag
SC003	SpyCatcher003 protein
ST003	SpyTag003 peptide
Gal-X	Galectin-X
L	Parts of the linker peptide of tandem repeat type Gal-4 and Gal-8
LGal-X	Linker located at the N-terminal site of the Gal-CRD
Gal-XL	Linker located at the N-terminal site of the Gal-CRD
Gal-XN	N-terminal CRD of Gal-X
Gal-XC	C-terminal CRD of Gal-X
eYFP	Enhanced yellow fluorescent protein
eGFP	Enhanced green fluorescent protein
DsRedM	Monomeric form of the red fluorescent protein DsRed
Sf-GFP	Superfolder-green fluorescent protein
Strep	Strep-tag II

The recombinant production of SpyCatcher/SpyTag-galectin fusion proteins was carried out in *E. coli* BL21 (DE3), *E. coli* Rosetta (DE3) pLysS, or *E. coli* Rosetta 2 (DE3) pLysS (Table S2) with cell yields of 13-24 g of cell wet weight per 1 L of cell culture (Table S3). All fusion proteins were purified by affinity chromatography (IMAC). Soluble protein fractions contained 3.6 - 6.2 mg g^{-1} of cell wet weight for SpyCatcher003-carrying galectin fusion proteins, except for the Gal-1C2S fusion protein, which had a significantly higher yield of 62.9 mg g^{-1} cells (Table S3). In contrast, the corresponding control proteins (without galectin CRD) exhibited a slightly higher yield of soluble protein of 14-47 mg g^{-1} cells. For SpyTag003 galectin fusion proteins, isolated protein amounts were in the range of 1.4 - 8.3 mg g^{-1} cells. Purification of Gal-3 resulted in a soluble protein fraction of 5.7 mg g^{-1} cells. These yields were consistent with those previously reported for SNAP-tagged galectin fusion proteins and are comparable to solely His_6-tagged galectins [8-10]. In control proteins, the higher soluble protein levels may be due to the facilitated recombinant protein expression in the absence of the Gal-3 domain in *E. coli*.

Table S2. *E.coli* strains used for recombinant expression of galectin constructs.

***E.coli* strain**	**Galectin construct**
BL21 (DE3)	pET28a::HYGal-3
	pETDuetI::strep-SC003-sfGFP
	pETDuetI::strep-ST003-sfGFP
Rosetta (DE3) pLysS	pETDuetI::HGal-3
	pET28a::HST003eYFPGal-3
Rosetta 2 (DE3) pLysS	pET17b::HSC003eYFPGal-3
	pET17b::HSC003DsRedMGal-3
	pET17b::HSC003DsRedMGal-1C2S
	pET17b::HSC003eGFPGal-8NL
	pET17b::HSC003eGFPLGal-8C
	pET17b::HSC003mCherryGal-4NL
	pET17b::HSC003mCherryLGal-4C
	pET17b::HSC003DsRedM
	pET17b::HSC003eGFP
	pET17b:HSC003mCherry
	pET17b:HSC003eYFP
	pET28a:HST003eYFP
	pET17b::HSC003Gal-3
	pET28a::HST003Gal-3

Table S3. Protein molecular weights (M_W).

Protein	**Abbreviation**	**M_W [kDa]**	**Cell yield [g L^{-1}]**	**Protein/ cell wet weight [mg g^{-1}]**
His_6SpyCatcher003eYFPGal-3	HSC003eYFPGal-3	67.2	16	3.7
His_6SpyCatcher003Gal-3	HSC003Gal-3	39.8	18.9	3.6
His_6eYFPGal-3	HeYFPGal-3	56.0	13	3.7
His_6SpyCatcher003eYFP	HSC003eYFP	41.7	14.8	30.5
His_6SpyTag003eYFPGal-3	HST003eYFPGal-3	57.5	14.5	1.4
His_6SpyTag003Gal-3	HST003Gal-3	30.5	12.9	5.2
His_6SpyTag003eYFP	HST003eYFP	31.4	13.4	8.3
His_6SpyCatcher003DsRedMGal-3	HSC003DsRedMGal-3	66.0	16.7	7.5
His_6Gal-3	HGal-3	28.0	14.5	5.7
His_6SpyCatcher003DsRedMGal-1C2S	HSC003DsRedMGal-1C2S	54.6	17.3	62.9
His_6SpyCatcher003DsRedM	HSC003DsRedM	40.5	24.4	46.9
His_6SpyCatcher003mCherryGal-4NL	HSC003mCherryGal-4NL	58.7	15.6	4.9
His_6SpyCatcher003mCherryLGal-4C	HSC003mCherryLGal-4C	57.8	19.2	5.4
His_6SpyCatcher003mCherry	HSC003mCherry	41.4	16	44.4
His_6SpyCatcher003eGFPGal-8NL	HSC003eGFPGal-8NL	59.4	18.1	4.1
His_6SpyCatcher003eGFPLGal-8C	HSC003eGFPLGal-8C	56.9	16.6	6.2
His_6SpyCatcher003eGFP	HSC003eGFP	42.1	12.8	13.5
Strep-SC003-sfGFP	-	44.0	19.4	0.8
Strep-ST003-sfGFP	-	33.8	16.6	1.0

SDS-PAGE analysis of the HSC003eYFPGal-3 IMAC eluate exhibited a predominant band corresponding to the full fusion protein (67.2 kDa) and protein bands ranging between 50 and 60 kDa, which were subsequently removed after ASF affinity chromatography (Fig. S1A). The presence of additional protein bands in the IMAC eluate correspond to N-terminal protein fragments and can be attributed to the respective fusion partners and a non-specific protein fragmentation during the purification process, as previously discussed [7]. In the case of HST003eYFPGal-3, an almost pure protein fraction was already evident during the IMAC purification (57.5 kDa) indicating a reduced susceptibility to fragmentation due to the small size of the SpyTag (Fig. S1B).

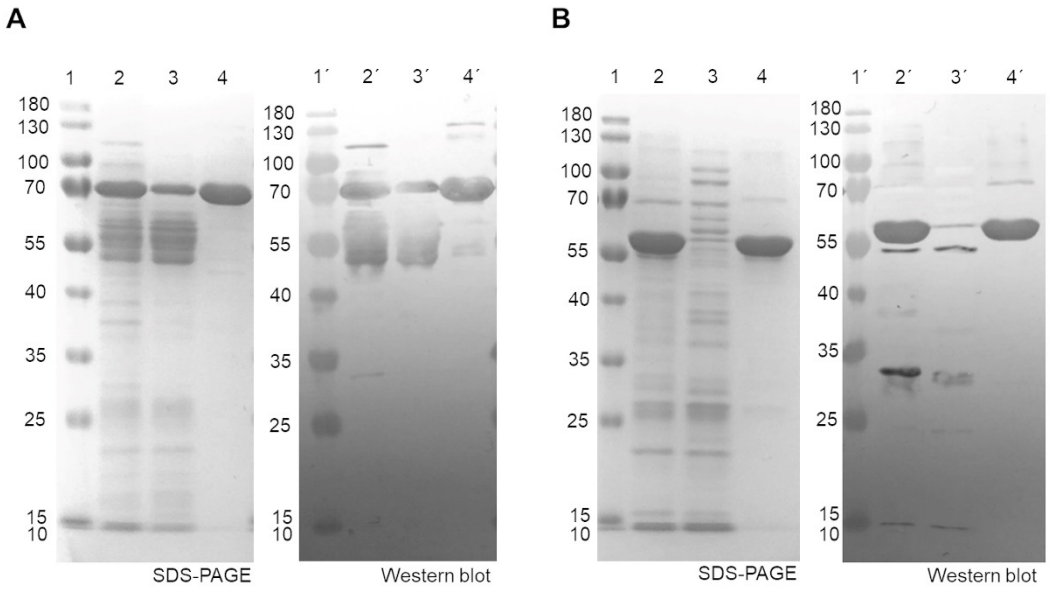

Figure S1. SDS-PAGE and Western blot analysis of SpyCatcher003- and SpyTag003-galectin fusion proteins after IMAC purification. **A**: HSC003eYFPGal-3 (M_W 67.2 kDa); **B**: HST003eYFPGal-3 (M_W: 57.5 kDa). 1/1´: Molecular weight standard 10-180 kDa; 2/2´: IMAC eluate; 3/3´: Wash fraction fine purification; 4/4´: Eluate fine purification. Running conditions: 12% reducing gel; 5 µg protein/lane; 200 V (const.); 60 min; Coomassie Blue stain; Proteins in Western blot were detected with an anti-His_6-tag antibody.

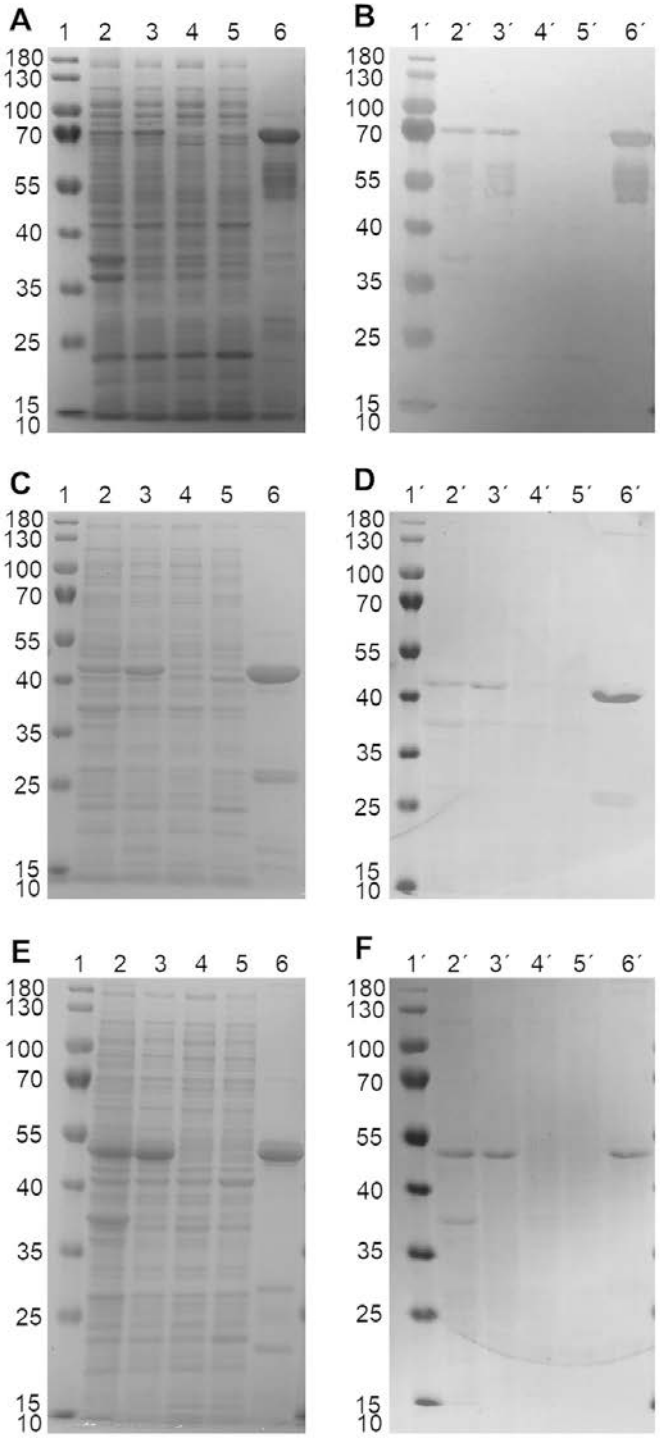

Figure S2. SDS-PAGE and Western blot analysis SpyCatcher003 Gal-3 fusion proteins after IMAC purification. For binding analysis, the galectins were further purified with ASF affinity resin. **A**: SDS-PAGE HSC003eYFPGal-3 (67.2 kDa); **B**: Western blot HSC003eYFPGal-3 (His_6-tag detection); **C**: SDS-PAGE HSC003Gal-3 (39.8 kDa); **D**: Western blot HSC003Gal-3 (SpyCatcher003 detection); **E**: SDS-PAGE HSC003eYFP (41.7 kDa); **F**: Western blot HSC003eYFP (SpyCatcher003 detection). 1/1´: Molecular weight standard 10-180 kDa; 2/2´: Pellet; 3/3`: Crude extract; 4/4´: Flow through; 5/5´: Wash step; 6/6`: Eluate. The proteins were purified using IMAC. Fractions of each purification step were pooled and subsequently applied to a 12% reducing gel (200 V (const.), 60 min, Coomassie Blue stain). In the Western blot, the proteins were detected either with an anti-His_6-antibody or with an anti-SpyCatcher-antibody.

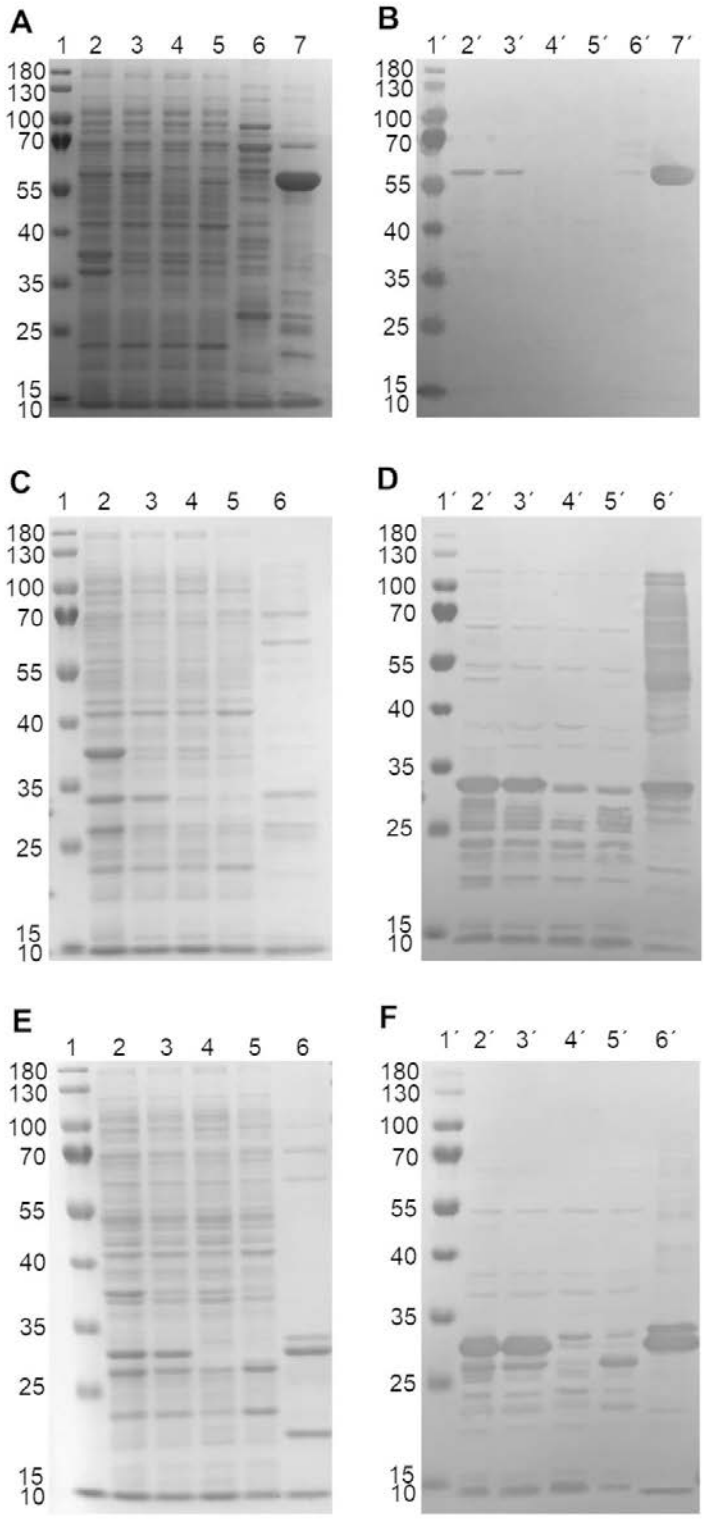

Figure S3. SDS-PAGE and Western blot analysis of SpyTag003 Gal-3 fusion proteins after IMAC purification (for binding analysis, the galectins were further purified with ASF affinity resin). **A**: SDS-PAGE HST003eYFPGal-3 (57.5 kDa); **B**: Western blot HST003eYFPGal-3; **C**: SDS-PAGE HST003Gal-3 (30.5 kDa); **D**: Western blot HST003Gal-3; **E**: SDS-PAGE HST003eYFP (31.4 kDa); **F**: Western blot HST003eYFP. 1/1´: Molecular weight standard 10-180 kDa; 2/2´: Pellet; 3/3`: Crude extract; 4/4´: Flow through; 5/5´: Wash step; 6/6`: Eluate. The proteins were purified using IMAC. Fractions of each purification step were pooled and subsequently applied to a 12% reducing gel (200 V (const.), 60 min, Coomassie Blue stain). In the Western blot, the proteins were detected with an anti-His_6 antibody.

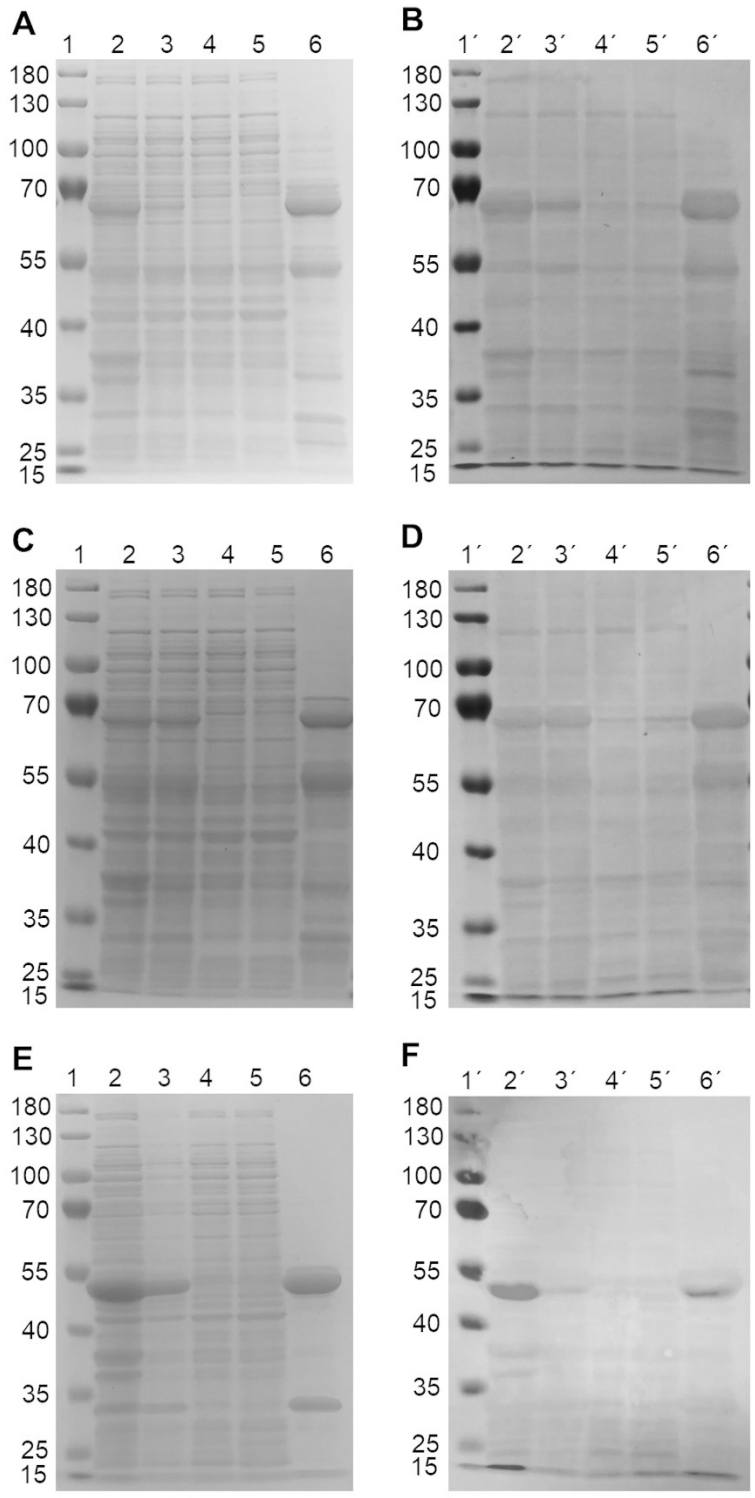

Figure S4. SDS-PAGE and Western blot analysis of SpyCatcher003 Gal-4 fusion proteins and corresponding control protein after IMAC purification. **A**: SDS-PAGE HSC003mCherryGal-4NL (58.7 kDa); **B**: Western blot HSC003mCherryGal-4NL; **C**: SDS-PAGE HSC003mCherryLGal-4C (57.8 kDa); **D**: Western blot HSC003mCherryLGal-4C; **E**: SDS-PAGE HSC003mCherry (41.4 kDa); **F**: Western blot HSC003mCherry. 1/1´: Molecular weight standard 10-180 kDa; 2/2´: Pellet; 3/3`: Crude extract; 4/4´: Flow through; 5/5´: Wash step; 6/6`: Eluate. The proteins were purified using IMAC. Fractions of each purification step were pooled and subsequently applied to a 10% reducing gel (200 V (const.), 60 min, Coomassie Blue stain). In the Western blot, the proteins were detected with an anti-SpyCatcher antibody.

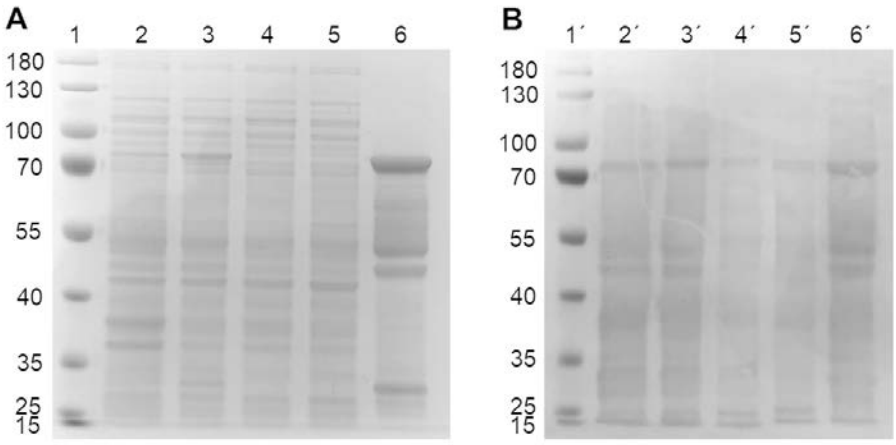

Figure S5. SDS-PAGE and Western blot analysis of HSC003DsRedMGal-3 after IMAC purification. **A**: SDS-PAGE HSC003DsRedMGal-3 (66 kDa); **B**: Western blot HSC003DsRedMGal-3. 1/1´: Molecular weight standard 10-180 kDa; 2/2´: Pellet; 3/3`: Crude extract; 4/4´: Flow through; 5/5´: Wash step; 6/6`: Eluate. The proteins were purified using IMAC. Fractions of each purification step were pooled and subsequently applied to a 10% reducing gel (200 V (const.), 60 min, Coomassie Blue stain). In the Western blot, the protein was detected with an anti-SpyCatcher antibody.

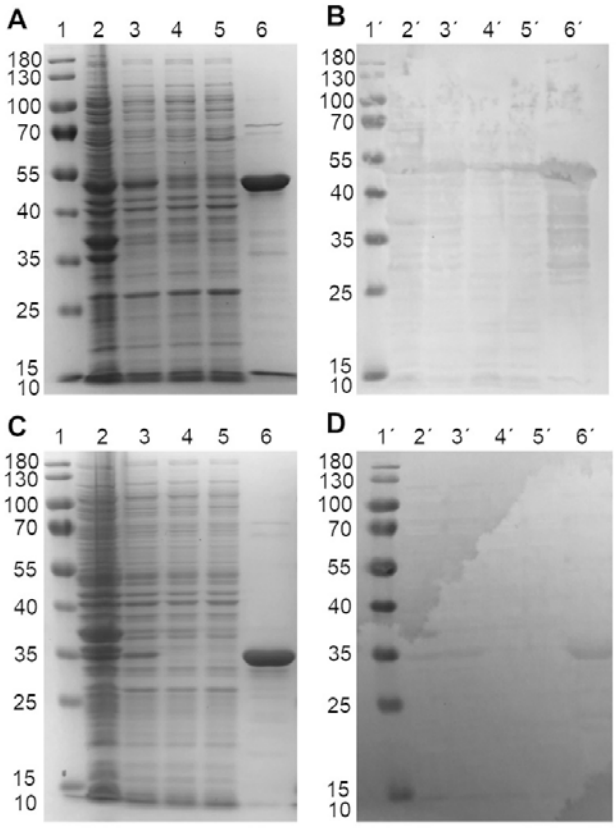

Figure S6. SDS-PAGE and Western blot analysis purity of proteins strep-SC003-sfGFP and strep-ST003-sfGFP. **A**: SDS-PAGE strep-SC003-sfGFP (44 kDa); **B**: Western blot strep-SC003-sfGFP; **C**: SDS-PAGE strep-ST003-sfGFP (33.8 kDa); **D**: Western blot strep-ST003-sfGFP. 1/1´: Molecular weight standard 10-180 kDa; 2/2´: Pellet; 3/3`: Crude extract; 4/4´: Flow through; 5/5´: Wash step; 6/6`: Eluate. The proteins were purified using Strep-Tactin XT. Fractions of each purification step were gathered and subsequently applied to a 12% reducing gel (200 V (const.), 60 min, Coomassie Blue stain). In the Western blot, the proteins were detected with an anti-SpyCatcher antibody (**B**) and an anti-strepTag-antibody (**D**).

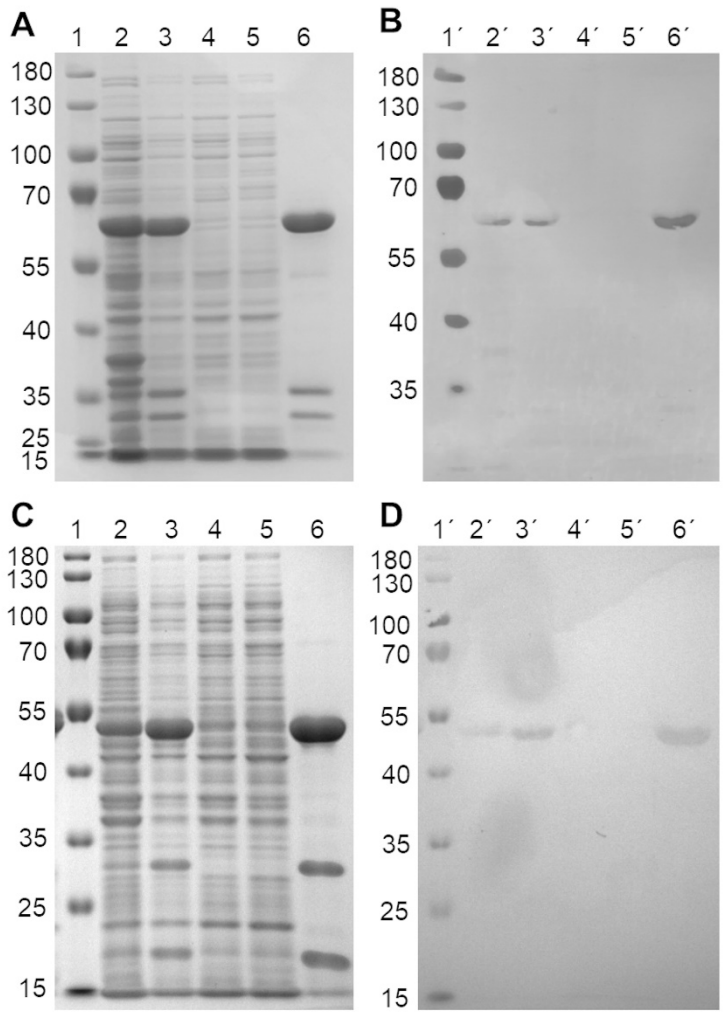

Figure S7. SDS-PAGE and Western blot analysis of SpyCatcher003-carrying Gal-1 fusion proteins and corresponding control protein after IMAC purification. **A**: SDS-PAGE HSC003DsRedMGal-1C2S (54.6 kDa); **B**: Western blot HSC003DsRedMGal-1C2S; **C**: SDS-PAGE HSC003DsRedM (40.5 kDa); **D**: Western blot HSC003DsRedM. 1/1´: Molecular weight standard 10-180 kDa; 2/2´: Pellet; 3/3`: Crude extract; 4/4´: Flow through; 5/5´: Wash step; 6/6`: Eluate. The proteins were purified using IMAC. Fractions of each purification step were gathered and subsequently applied to a 10% reducing gel (200 V (const.), 60 min, Coomassie Blue stain). In the Western blot, the proteins were detected with an anti-SpyCatcher antibody.

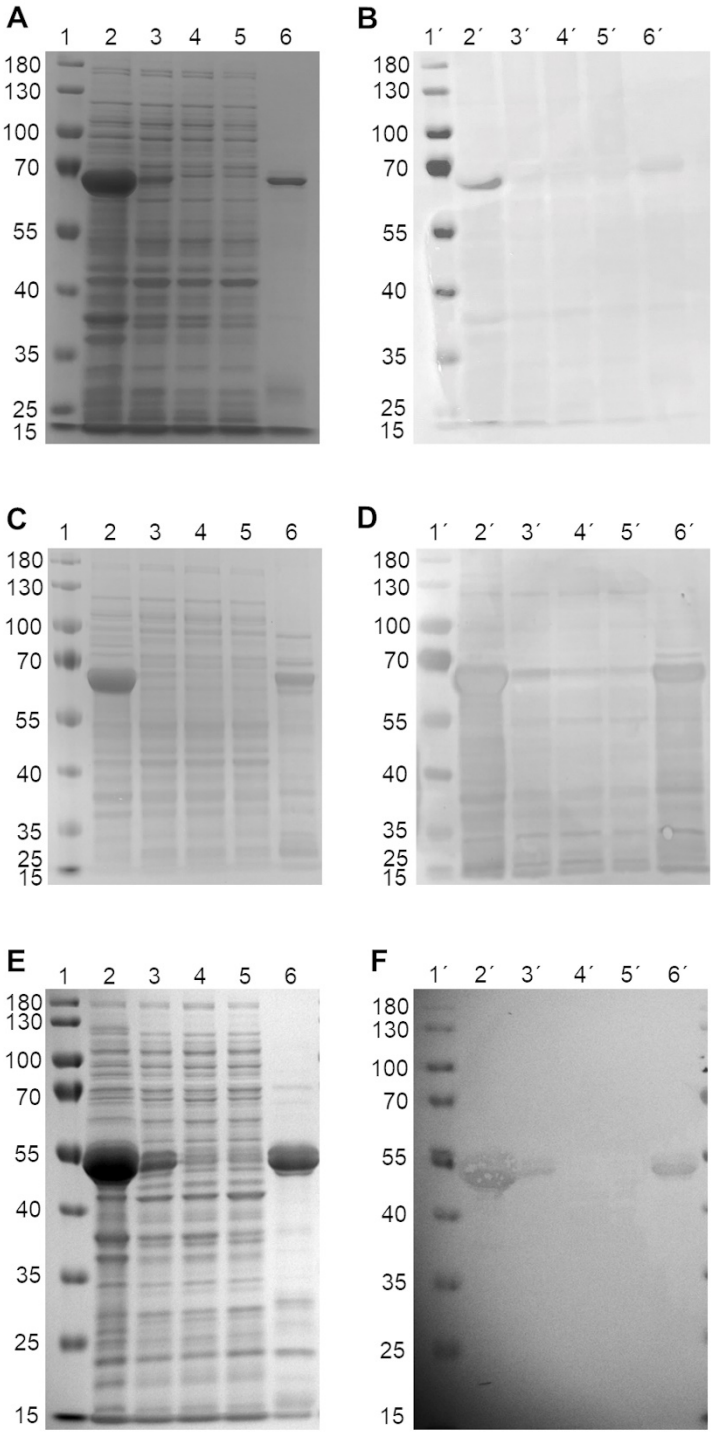

Figure S8. SDS-PAGE and Western blot analysis of SpyCatcher003 Gal-8NL and LGal-8C fusion proteins and corresponding control protein after IMAC purification. **A**: SDS-PAGE HSC003eGFPGal-8NL (59.4 kDa); **B**: Western blot HSC003eGFPGal-8NL; **C**: SDS-PAGE HSC003eGFPLGal-8C (56.9 kDa); **D**: Western blot HSC003eGFPLGal-8C; **E**: SDS-PAGE HSC003eGFP (42.1 kDa); **F**: Western blot HSC003eGFP. 1/1´: Molecular weight standard 10-180 kDa; 2/2´: Pellet; 3/3`: Crude extract; 4/4´: Flow through; 5/5´: Wash step; 6/6`: Eluate. Fractions of each purification step were gathered and subsequently applied to a 10-12% reducing gel (200 V (const.), 60 min, Coomassie Blue stain). In the Western blot, the proteins were detected with an anti-SpyCatcher antibody.

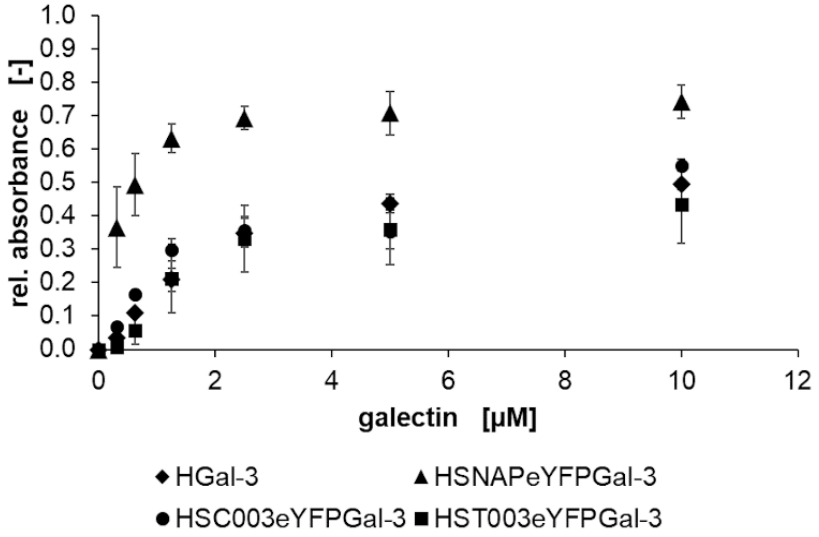

Figure S9. Gal-3 binding to ASF: SNAP-tag, SpyCatcher003, and SpyTag003 Gal-3 fusion proteins compared with His_6-tagged Gal-3. The binding is shown for HSNAPeYFPGal-3 (▲), HSC003eYFPGal-3 (●), HST003eYFPGal-3 (■), and HGal-3 (◆). Galectin binding was identified using a peroxidase-conjugated anti-His_6 antibody. The mean signal from three data points was determined by the conversion of TMB substrate. Standard deviations are represented as error bars.

Table S4. Apparent K_D values and binding efficiencies of Gal-3 fusion proteins and His_6-tagged Gal-3. Values are based on *in vitro* binding of ASF. Data were computed by non-linear regression. The binding efficiencies (*BE*) were calculated as the ratios of B_{max} and K_D.

Galectin	Apparent K_D [µM]	B_{max} [-]	*BE* [$µM^{-1}$]
HGal-3	2.3 ± 0.3	0.7	0.3
HSNAPeYFPGal-3	0.3 ± 0.1	0.7	2.3
HSC003eYFPGal-3	2.0 ± 0.5	0.7	0.3
HST003eYFPGal-3	2.0 ± 0.7	0.7	0.3

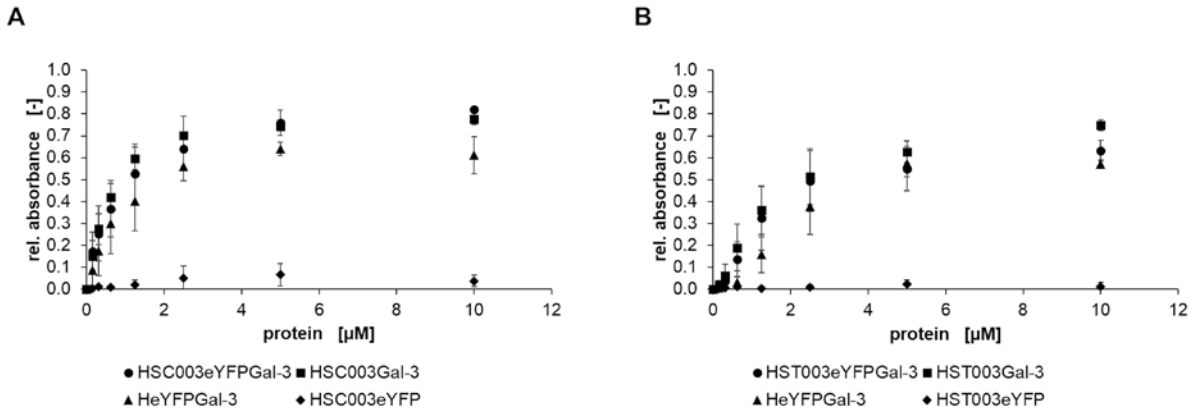

Figure S10. Binding of Gal-3 fusion proteins. *In vitro* binding to ASF is shown for **A:** SpyCatcher003 fusion proteins (HSC003eYFPGal-3 (●); HSC003Gal-3 (■); HeYFPGal-3 (▲), HSC003eYFP (◆)) and **B:** SpyTag003 fusion proteins (HST003eYFPGal-3 (●); HST003Gal-3 (■); HeYFPGal-3 (▲), HST003eYFP (◆)). The mean signal from three data points was determined by the conversion of TMB substrate. Standard deviations are represented as error bars.

Table S5. ASF binding assay of different Gal-3 SpyCatcher and SpyTag fusion constructs. K_D values were calculated through non-linear regression. The binding efficiencies (*BE*) were calculated as the ratios of B_{max} and K_D.

Protein	**Apparent K_D [µM]**	**B_{max} [-]**	***BE* [µM^{-1}]**
HSC003eYFPGal-3	0.8 ± 0.2	0.9 ± 0.1	1.0
HSC003Gal-3	0.6 ± 0.1	0.8 ± 0.0	1.4
HeYFPGal-3	0.9 ± 0.3	0.7 ± 0.1	0.8
HST003eYFPGal-3	2.1 ± 0.7	0.8 ± 0.1	0.4
HST003Gal-3	2.3 ± 0.5	0.9 ± 0.1	0.4
HeYFPGal-3	4.3 ± 1.5	0.9 ± 0.1	0.2

Table S6. Apparent K_D values of SpyCatcher003 and SpyTag003 galectin fusion proteins. The binding affinity of HSC003eYFPGal-3 and HST003eYFPGal-3 was tested with an *in vitro* binding assay on ASF at 7 different time points over 12 days. K_D values were calculated by non-linear fitting based on three data points. Errors indicate standard deviations. The binding efficiencies (*BE*) were calculated as the ratio of B_{max} and K_D.

	HSC003eYFPGal-3			**HST003eYFPGal-3**		
Day	K_D [µM]	B_{max} [-]	*BE* [µM^{-1}]	K_D [µM]	B_{max} [-]	*BE* [µM^{-1}]
1	2.59 ± 0.90	0.70 ± 0.08	0.27	0.79 ± 0.22	0.74 ± 0.05	0.94
2	0.45 ± 0.13	0.63 ± 0.04	1.39	0.34 ± 0.09	0.67 ± 0.03	1.97
3	0.60 ± 0.12	0.65 ± 0.03	1.08	0.69 ± 0.19	0.68 ± 0.04	0.98
4	1.19 ± 0.47	0.69 ± 0.07	0.58	0.62 ± 0.19	0.67 ± 0.05	1.08
5	1.35 ± 0.39	0.71 ± 0.06	0.52	1.01 ± 0.32	0.71 ± 0.06	0.70
10	0.86 ± 0.15	0.74 ± 0.03	0.86	0.88 ± 0.32	0.70 ± 0.06	0.80
12	0.73 ± 0.10	0.69 ± 0.02	0.94	0.57 ± 0.06	0.71 ± 0.02	1.25

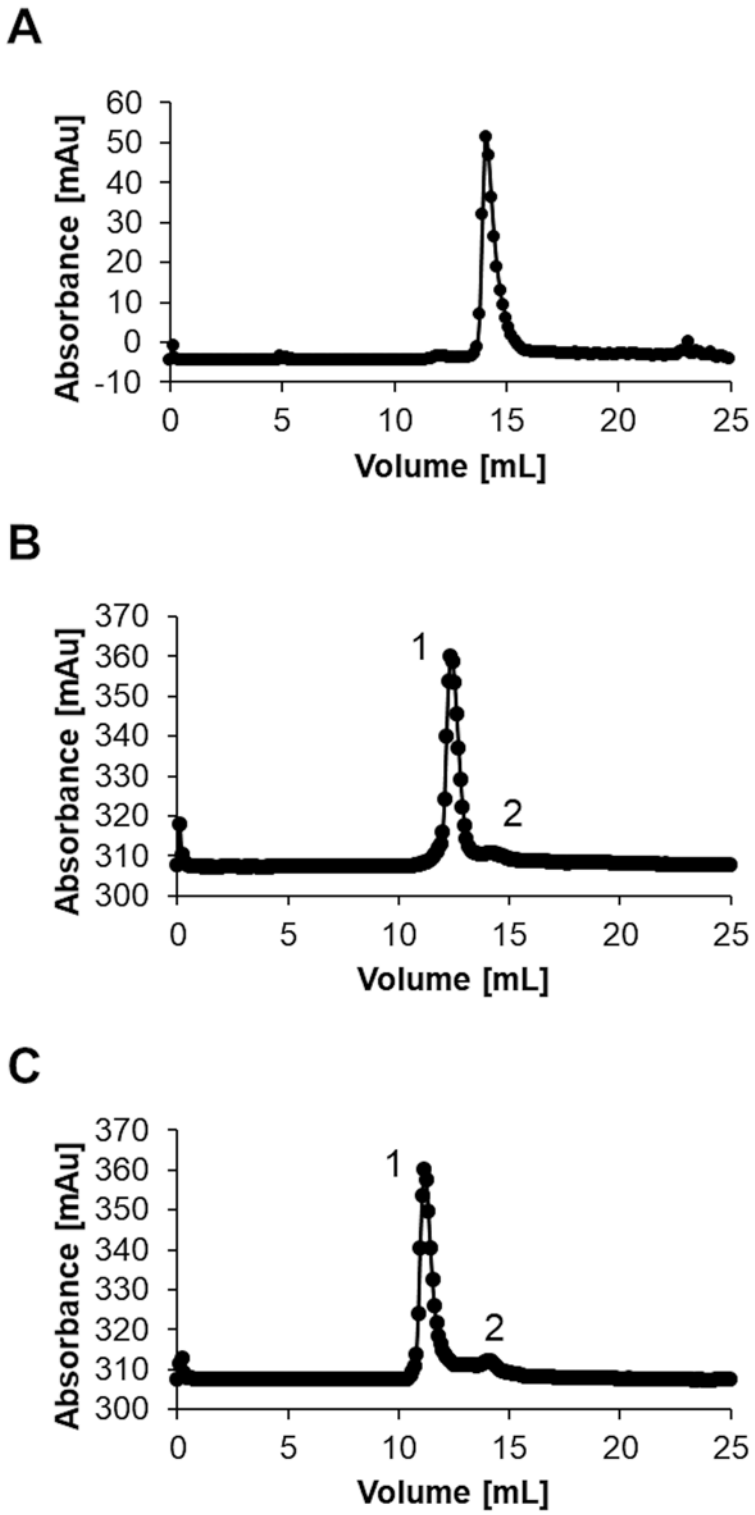

Figure S11. Elution profiles of size exclusion chromatography (SEC). Galectin fusion proteins HSC003eYFPGal-3 and HST003eYFPGal-3 were purified by IMAC and lactose-agarose chromatography. The SC-ST-Gal-3 conjugate was formed by incubating 20 µM of each galectin fusion protein in a rotary shaker for 1 h at 4 °C and 20 rpm. 200 µL of each sample was applied onto a Superdex Increase 200 10/300 GL column using a flow rate of 0.75 mL min^{-1}. The molecular weights were calculated by linear regression of standard proteins. **A**: HST003eYFPGal-3 (20 µM); **B**: HSC003eYFPGal-3 (20 µM); **C**: SC-ST-Gal-3 conjugate (10 µM).

A

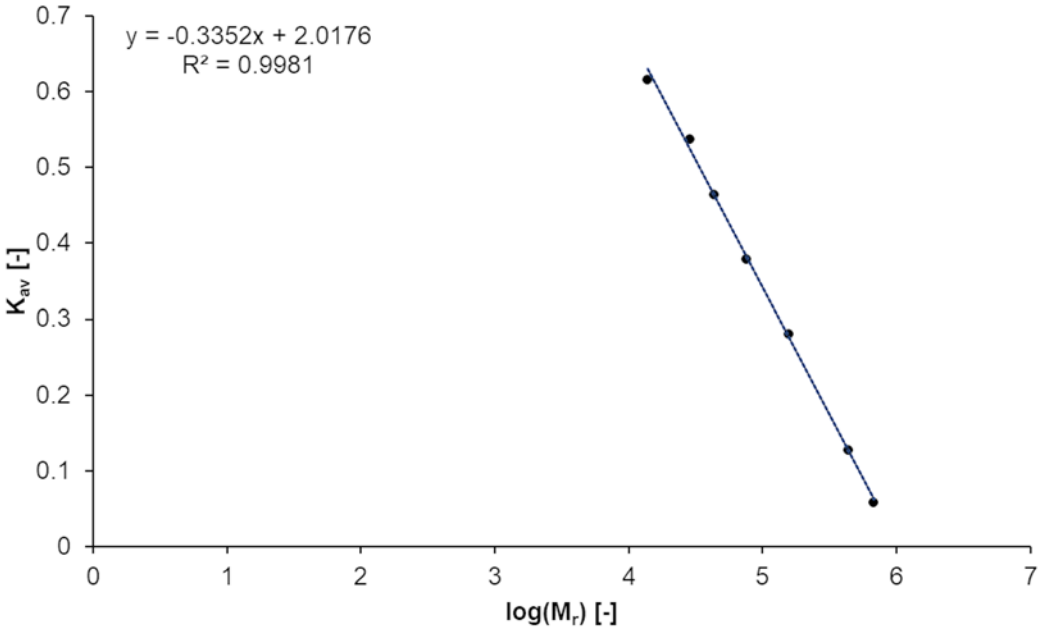

B

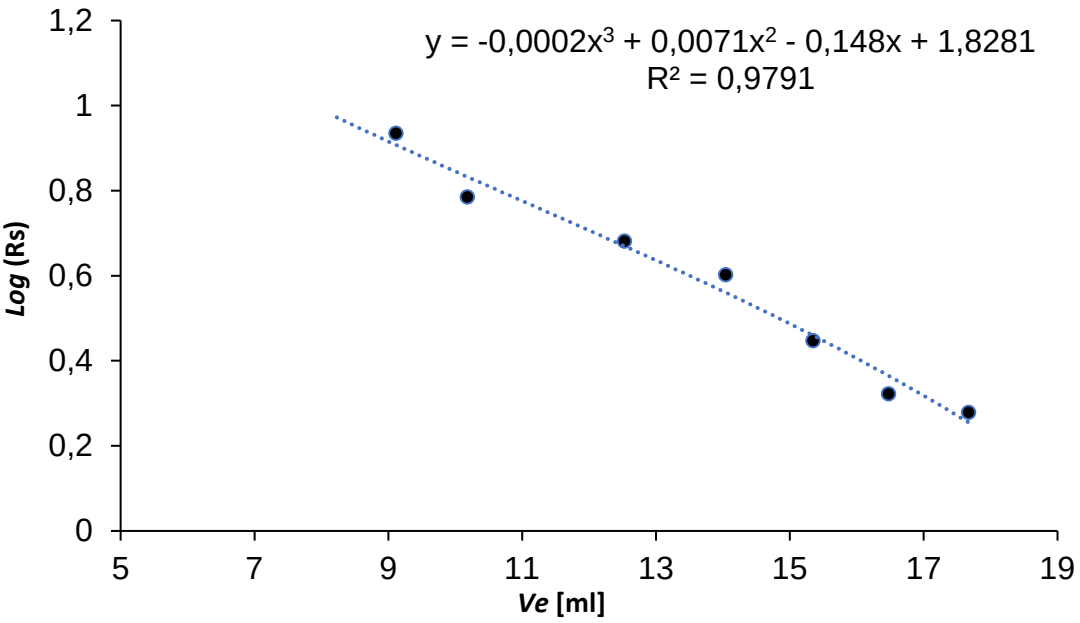

Figure S12. A. SEC calibration curve (thyroglobulin 669 kDa; ferritin 440 kDa; aldolase 158 kDa; conalbumin 75 kDa; ovalbumin 44 kDa; carbonic anhydrase 29 kDa; ribonuclease 13.7 kDa). **B**. SEC calibration for the determination of Stokes diameters (D_S) based on the Stokes radii of the standard proteins.

Table S7. Molecular weights (M_W) and Stokes diameters (D_S) of Gal-3 fusion proteins and SC-ST-Gal-3 conjugate calculated by SEC. The theoretical molecular weights (M_W) were calculated based on the amino acid sequence and correspond to the monomeric form. M_W (SEC) was calculated using calibration Fig. S12 A. D_S (SEC) was calculated using calibration Fig. S12 B.

Protein:	**M_W (theor.) [kDa]:**	**M_W (SEC) [kDa]:**	**D_S (SEC) [nm]:**
HST003eYFPGal-3	57.5	77.3	7.9
HSC003eYFPGal-3	67.2	Peak 1: 165.7	10.2
		Peak 2: 73.7	7.8
SC/ST-Gal-3 conjugate	124.7	Peak 1: 287.5	12.2
		Peak 2:78.4	7.9

Dynamic Light Scattering (DLS)

DLS measurements were burdened by number fluctuations possibly caused by low concentration of samples (fast diffusive modes noise in autocorrelation function) and by bigger particles in solutions (noise in slow diffusive modes and nonlinear decay). The data are therefore presented as intensity and volume weighted distributions with careful evaluation of z-average and overall polydispersity. For HST003YFPeGal-3 construct, the data seem reliable and can be interpreted as volume-weighted distribution at 58.1 nm. The same applies for the SC-ST conjugate, which, although it has a bimodal intensity weighted distribution, it can be evaluated as a single peak at 11.0 nm where we could neglect the large diameter population at 239 nm because the light scattering intensity of particles is proportional to the sixth power of its diameter. In the case of HSCY003YFPeGal-3, the intensity-weighted distribution result 84.0 nm is largely overestimated due to the noise factor of the whole autocorrelation curve. The cumulant fit produced an underestimated Z-average at 4.4 nm, which tries to compensate for the large noise in fast diffusion modes. Using GPC as a complementary measurement helps us in the interpretation of the particles where the closest result is volume weighed distribution D_h = 22.0 nm which indicates 2fold – 4fold oligomers, but here we have to still keep in mind that these results has a high margin of error given by the noisy correlation.

Table S8: Cumulant fit average diameter $Z_{(avg)}$, polydispersity index *PDI* with intensity and volume weighted Hydrodynamic Radii D_h and percentual content for each peak of samples HST003eYFPGal-3, HSC003YFPGal-3 and SC-ST-Gal-3 conjugate.

Gal-3 construct:	**$Z_{(avg)}$ [nm]**	**Peak #**	**Intensity**		**Volume**		**PDI**	**Mass %**
			D_h [nm]	**%**	**D_h [nm]**	**%**		
HST003YFPe	50.2	1.	66.8	100	58.1	100	0.17	100
HSCY003YPe	4.4	1.	84.0	100	22.0	100	0.75	100
SC-ST conj.	29.8	1.	12.2	54.5	11.0	98.3	0.22	97.9
		2.	28.4	3.30	-	-		0.40
		3.	239	30.0	493	1.70	0.23	0.80

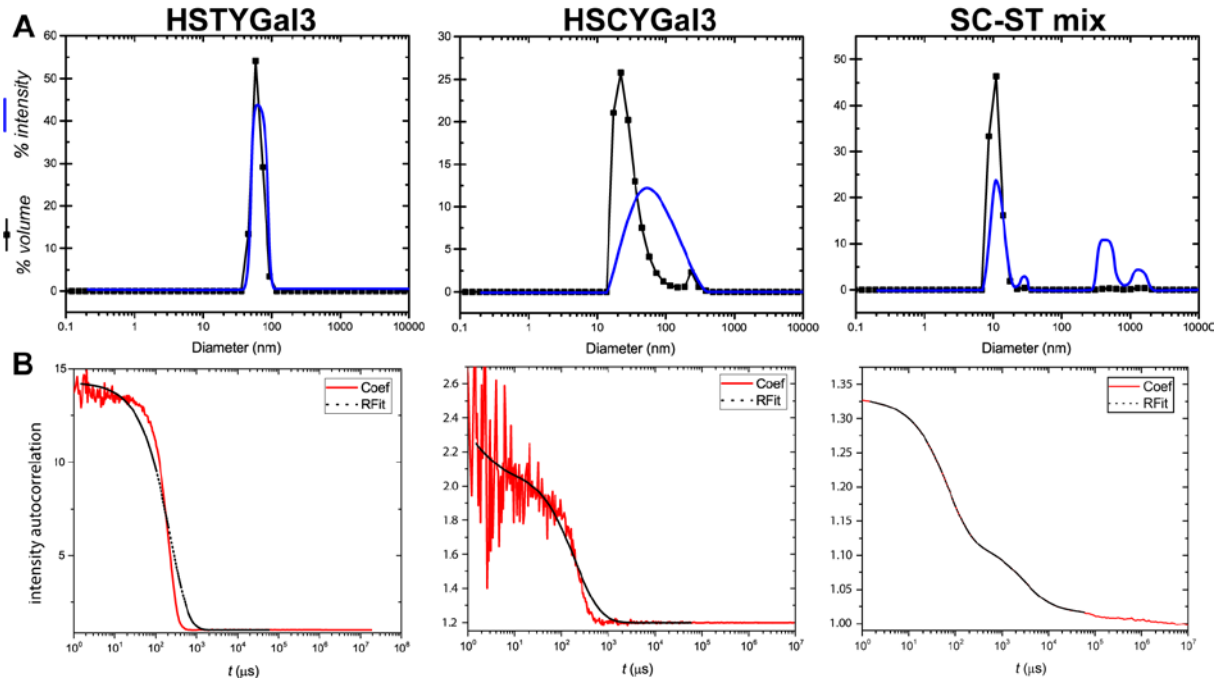

Figure S13. DLS results A) regularized autocorrelation fit: blue line represents intensity weighed distributions for galectin constructs and black line with full squares represents volume weighed distribution. B) Autocorrelation functions (red lines) for each galectin construct and respective regularized fits (black lines) for respective galectin fusion proteins.

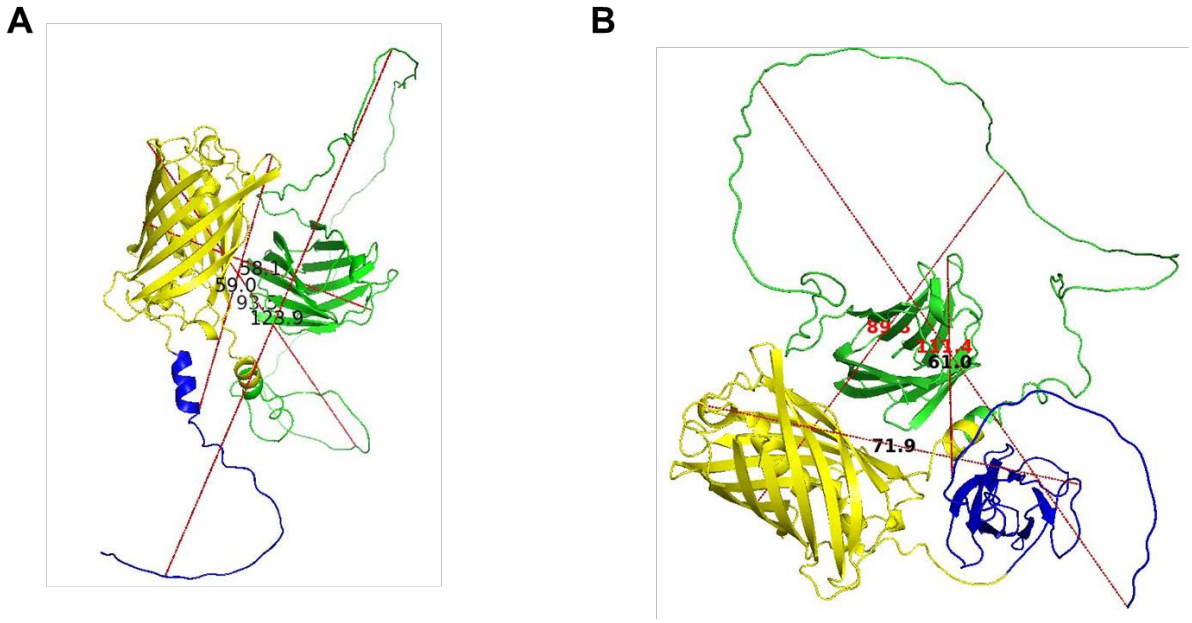

Figure S14. AlphaFold models of HST003eYFPGal-3 (**A**) and HSC003eYFPGal-3 (**B**). Blue: His_6-SpyTag003 or His_6-SpyCatcher003; Yellow: eYFP; Green; human Gal-3. The measurements between protein segments are given in angstroms (Å).

Application of Gal-3 fusion proteins for layering ECM glycoproteins

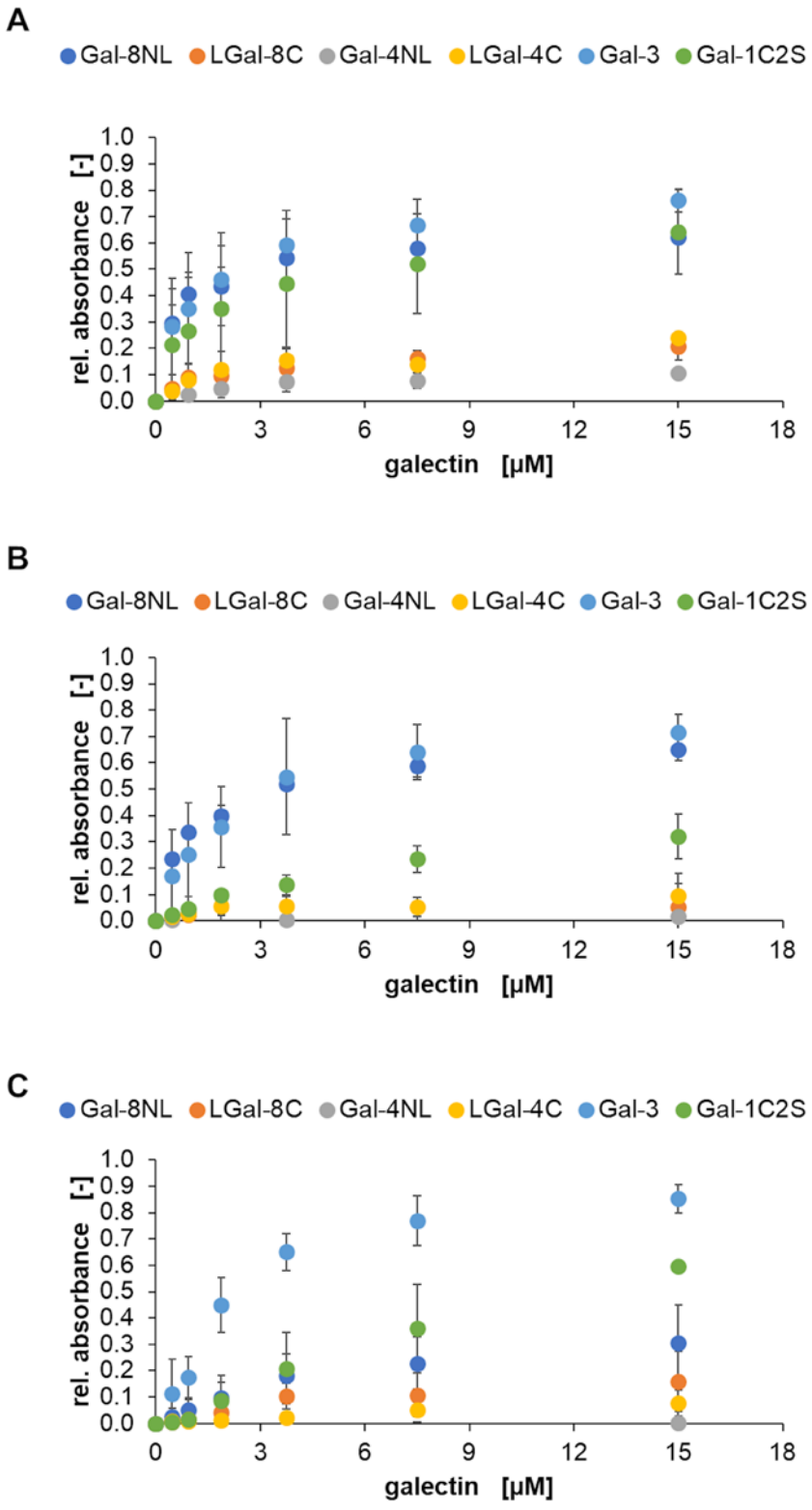

Figure S15. Binding of SpyCatcher galectin fusion proteins to glycoproteins. **A**: ASF; **B**: Fetuin; **C**: Laminin. The binding of HSC003DsRedMGal-1C2S (Gal-1C2S), HSC003eYFPGal-3 (Gal-3), HSC003mCherryGal-4NL (Gal-4NL), HSC003mCherryLGal-4C (LGal-4C), HSC003eGFPGal-8NL (Gal-8NL) and HSC003eGFPLGal-8C (LGal-8C) was investigated in an *in vitro* binding assay. Two technical replicates were measured in three independent experiments. Error bars indicate standard deviations.

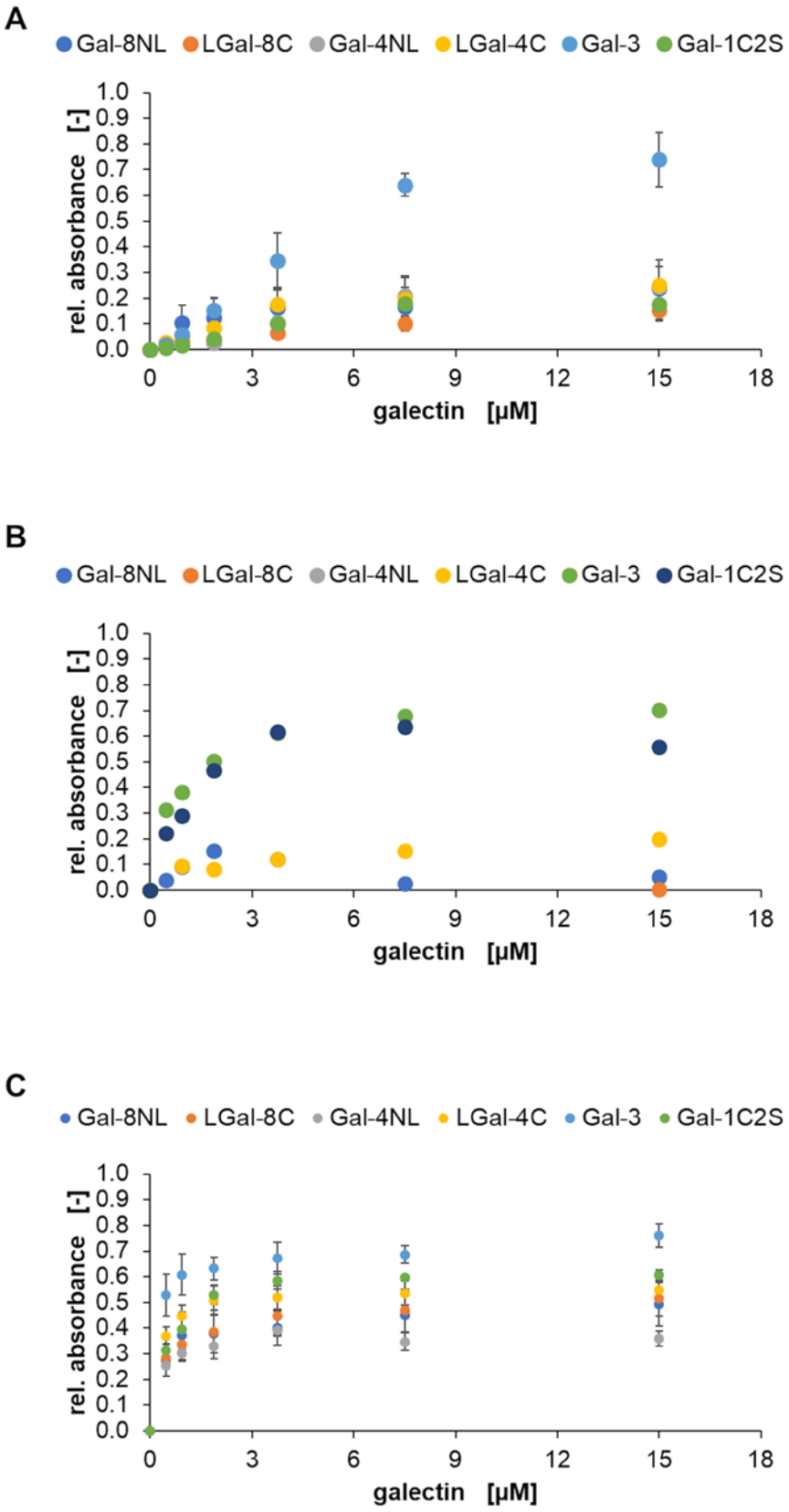

Figure S16. Binding behavior of SpyCatcher galectin fusion proteins on glycoproteins. **A**: Fibronectin; **B**: Collagen IV; **C**: Muc II. The binding of HSC003DsRedMGal-1C2S (Gal-1C2S), HSC003eYFPGal-3 (Gal-3), HSC003mCherryGal-4NL (Gal-4NL), HSC003mCherryLGal-4C (LGal-4C), HSC003eGFPGal-8NL (Gal-8NL) and HSC003eGFPLGal-8C (LGal-8C) was investigated in an *in vitro* binding assay. Two technical replicates were measured in three independent experiments. Error bars indicate standard deviations.

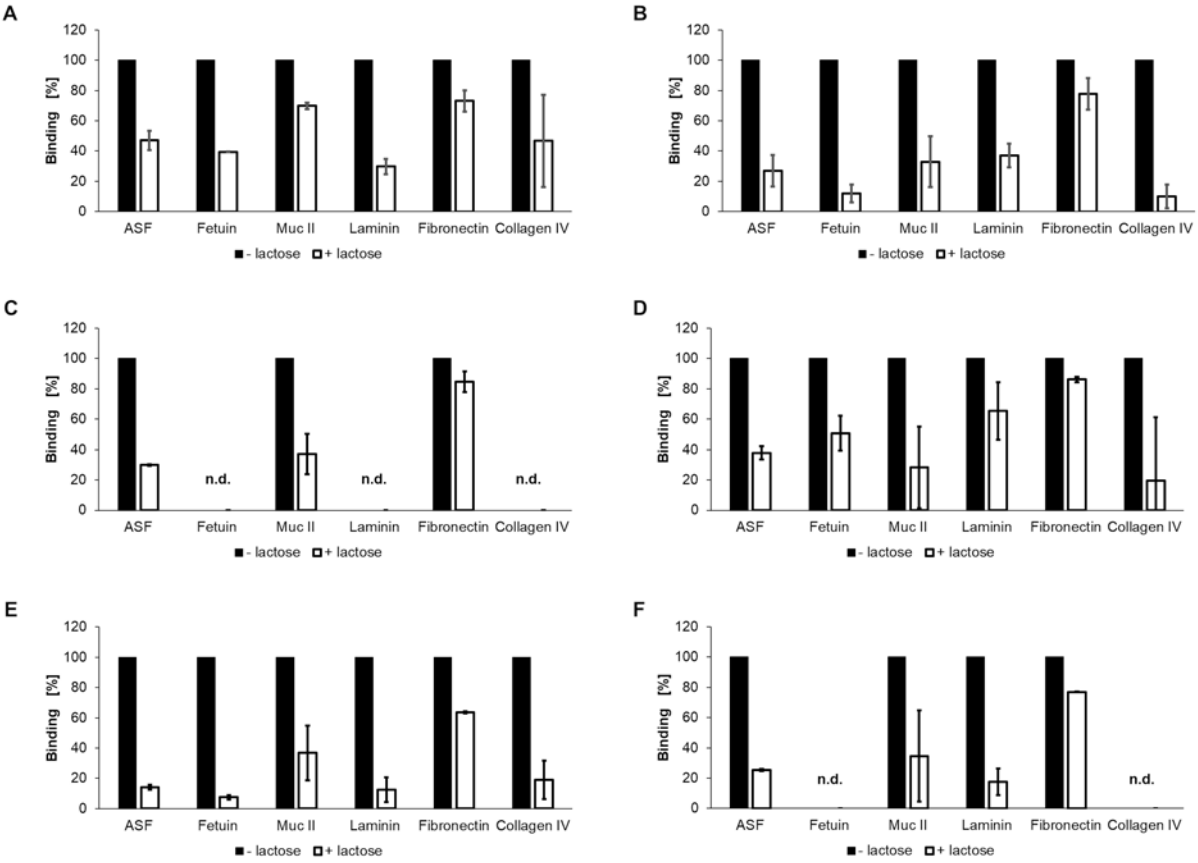

Figure S17. Inhibition of binding of SpyCatcher003 galectin fusion proteins to glycoproteins. The binding of galectins (30 µM) to glycoproteins was assessed in an *in vitro* binding assay, both with lactose (200 mM) and without lactose. The highest binding signal without lactose was set to 100% and residual binding in the presence of lactose was calculated relative to the highest signal without lactose (n.d.: not detected). **A:** HSC003DsRedMGal-1C2S; **B:** HSC003eYFPGal-3; **C:** HSC003mCherryGal-4NL; **D:** HSC003mCherryLGal-4C; **E:** HSC003eGFPGal-8NL; **F:** HSC003eGFPLGal-8C.

Binding of galectin fusion proteins to adenocarcinoma cell line DLD-1

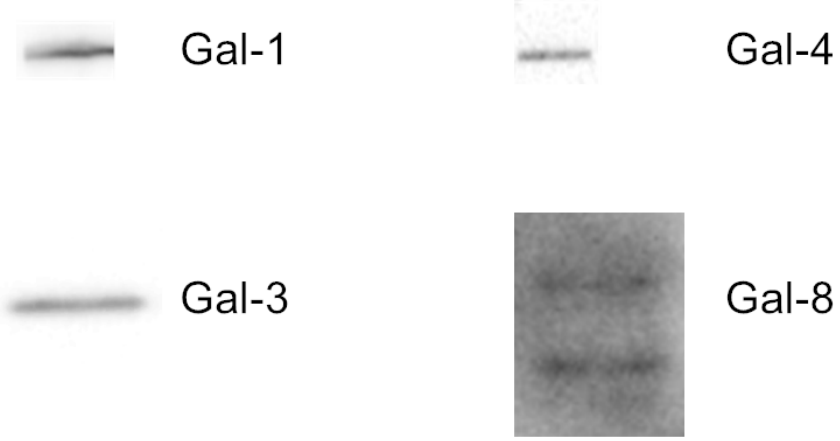

Figure S18. Western blot of Gal-1, Gal-3, Gal-4, and Gal-8 expression in DLD-1 cancer cells. Respective galectin bands corresponding to the right size (Gal-1: 15 kDa, Gal-3: 28 kDa, Gal-4: 36 kDa, Gal-8: 30 kDa dimer or 20 kDa monomer) were detected in all cases. In the case of Gal-8, the monomeric form is also visible (lower band).

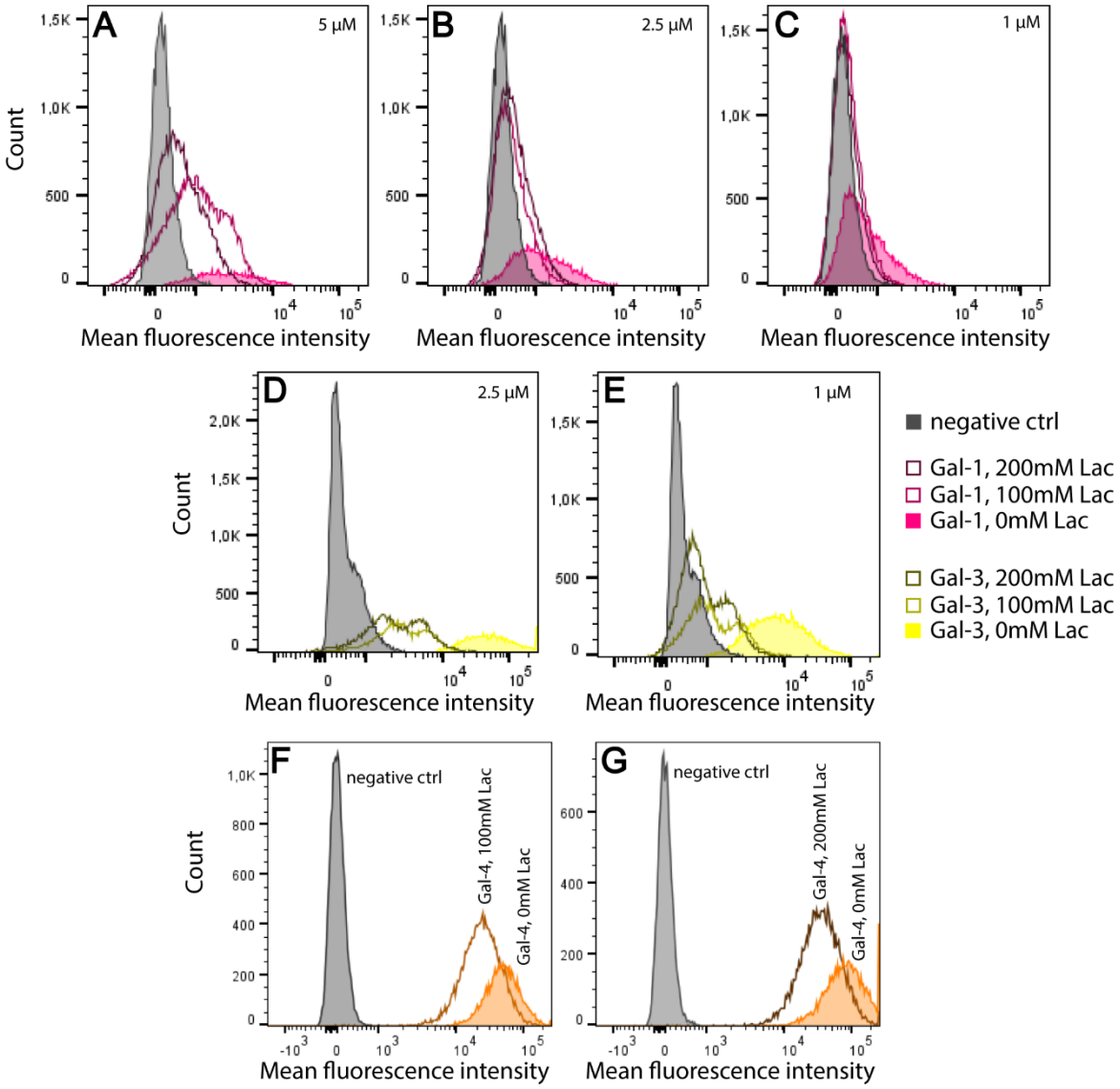

Figure S19: Overlay of representative flow cytometry histograms showing the binding of the SpyCatcher galectin fusion protein constructs to the DLD-1 cell surface in the presence of lactose (inhibitor). The binding of galectin constructs was determined by flow cytometry in the respective laser/detector configuration. Used molar concentrations of galectin constructs: HSC003DsRedMGal-1C2S: (**A**) 5 µM, (**B**) 2.5 µM, (**C**) 1 µM, HSC003eYFPGal-3: (**D**) 2.5 µM, (**E**) 1 µM, (**F**, **G**) HSC003mCherryGal-4NL 17.5 µM. Untreated cells are shown in grey.

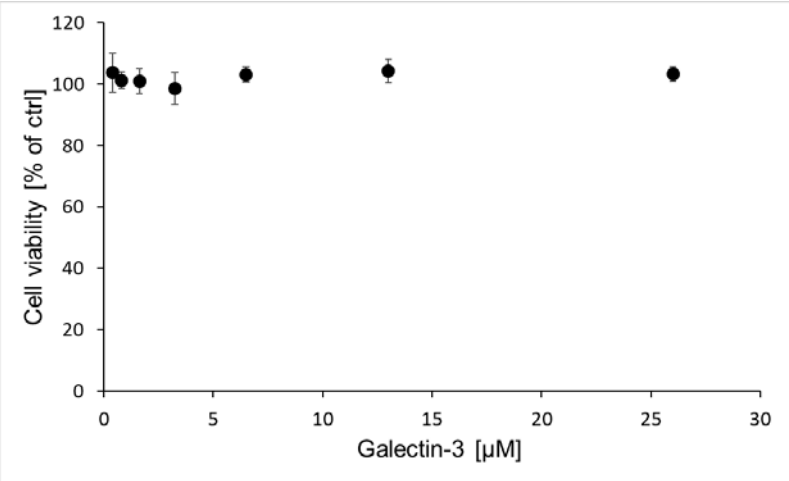

Figure S20. Cytotoxicity of recombinant HGal-3.

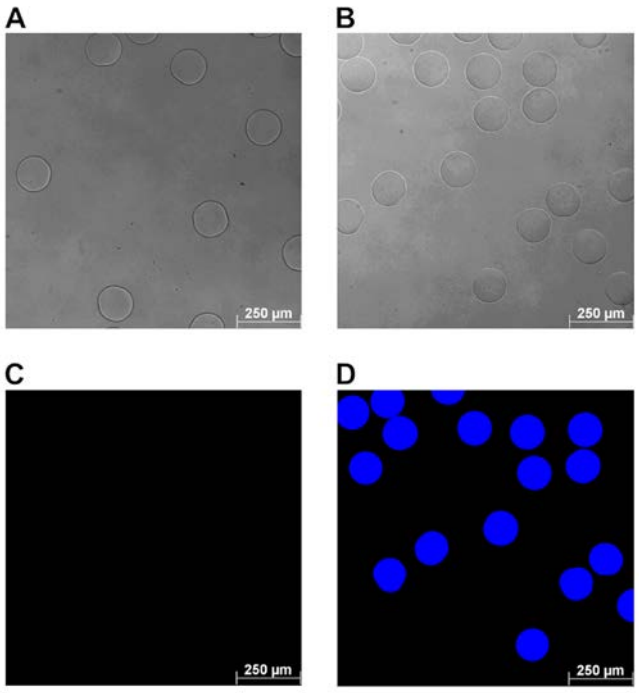

Figure S21. Microscopy images of microgels and analysis of SpyTag003 incorporation. After the synthesis of SpyCatcher003-presenting microgels, the incorporation of SpyTag003 was confirmed by fluorescamine staining of primary amines and subsequent fluorescence measurement. **A + C**: Non-functionalized microgels; **B + D**: SpyTag003-microgels: **A + B**: Microgels visualized with optical microscopy; **C + D**: Microgels visualized in blue channel (emission wavelength: 455-500 nm).

A

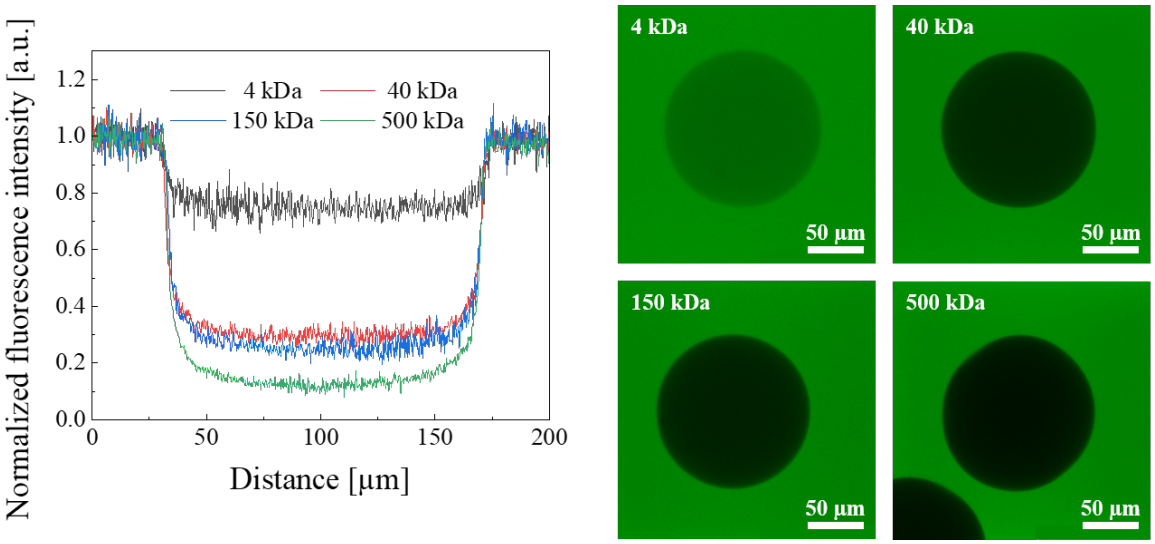

B

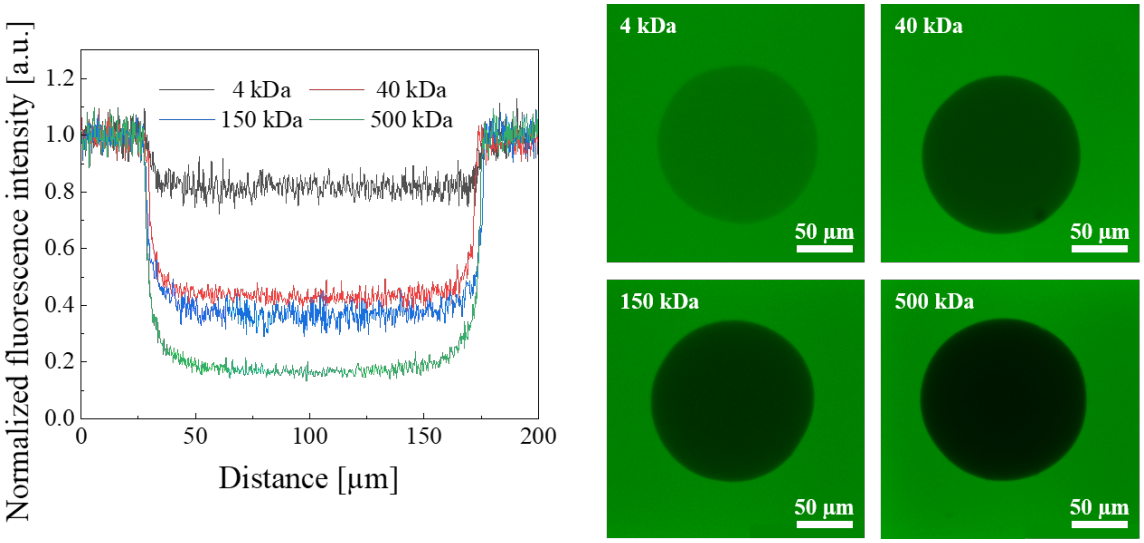

Figure S22. Investigation of the permeability through fluorescence intensity profiles of microgel cross-sections (left). The investigated confocal images are shown on the right. Before investigation with confocal microscopy, microgels were immersed in a 1 mg mL^{-1} FITC-dextran solution (4 to 500 kDa). **A**: SpyTag003-microgels; **B**: Non-functionalized microgels.